Proceedings of the ASME 2019
International Mechanical Engineering Congress and Exposition
IMECE2019
November 11-14, 2019, Salt Lake City, UT, USA

IMECE2019-10621

JOINING TECHNIQUES FOR NOVEL METAL POLYMER HYBRID HEAT EXCHANGERS

Gowtham Kuntumalla, Yuquan Meng, Manjunath Rajagopal, Ricardo Toro, Hanyang Zhao, Ho Chan Chang, Sreenath Sundar, Srinivasa Salapaka, Nenad Miljkovic, Chenhui Shao, Placid Ferreira, Sanjiv Sinha[1],
University of Illinois at Urbana-Champaign
Urbana, IL, USA

ABSTRACT

In the United States, over 50% of the unrecovered energy from industrial processes is in the form of low-grade heat (<220°C). Materials and maintenance costs of common heat exchangers are typically too high to justify their usage. Polymers, though more affordable, are usually unsuitable for HX applications due to their low thermal conductivity (~0.2 W/mK). Here, we show that metal-polymer hybrids may be attractive from both performance and cost perspectives. The use of polymers further increases the resistance to corrosion by sulfuric and carbonic acids often present in flue gases. An ongoing work explores different configurations of layered polyimide-copper macroscale hybrids for heat exchanger applications using numerical simulations. This paper explores a manufacturing pathway for producing such layered hybrid tubes that involves directly rolling and bonding tapes made of polymer and copper foil into tubes. A critical problem in the fabrication process is the bonding of metal and polymers. We explore approaches involving adhesives (epoxy, acrylic and silicone) for metal/polymer interfaces and direct welding (ultrasonic) for metal/metal interfaces that can be integrated into the manufacturing process. We report characterizations of the thermomechanical properties of these joining processes. This work paves the way for realizing cost-effective manufacturing of heat exchangers for low grade waste heat recovery.

Keywords: copper, polymer, polyimide, joining techniques, adhesives, dissimilar materials, heat exchangers, roll-to-roll process

NOMENCLATURE

Adh	Adhesive
Cu	Copper
HX	Heat Exchanger
M/M	Metal/Metal joint
M/P	Metal/Polymer joint
Poly	Polymer
l_{Cu}	Length of copper layer
l_o	Length of overlap
l_{poly}	Length of polymer layer
t_{Cu}	Thickness of copper layer
t_{poly}	Thickness of polymer layer
R2R	Roll to roll process
RSW	Resistance seam welding
USW	Ultrasonic welding

1. INTRODUCTION

Low-grade heat (<220 °C) comprises between 50 to 60% of the unrecovered energy from industrial processes [1]. Traditional all-metal heat exchangers (HX) are typically too expensive for such applications where the payback period is less than 3 years [2]. Further, corrosion from condensed sulfuric and carbonic acids at temperatures <150 °C create additional problems for metallic HX [3]. The use of polymers in low temperature HX can reduce costs and provide better resistance to corrosion. However, polymers remain unsuitable due to their low thermal conductivity (~0.2 W/m.K). The low conductivity leads to a high wall thermal resistance that limits the overall heat transfer coefficient.

Recent work has explored several approaches [4–9] for enhancing the thermal conductivity of polymers. Wang et al. [8] used high modulus, thin polymer fibers and measured thermal conductivity along the fibers. This approach is not beneficial in the case of heat exchangers due to the requirement of heat conduction in the transverse direction. Choy et al. [9] have proposed ultra-drawn polyethylene. Though the axial tensile modulus and axial thermal conductivity increase in this approach, properties along the transverse directions suffer. Roy et al. [7] demonstrated improved thermal conductivity of thin film polymer brushes in the cross-plane direction but the extremely low thickness (< 40nm) of the material limits its use in practical applications. The more common approach of [5,10] dispersing metal particles during polymerization of thick

[1] Corresponding author: sanjiv@illinois.edu

polymers (> 1mm) yields high thermal conductivity (~10-12 W/m.K). These metal-polymer micro-mixtures show as high as ~60% reduction in tensile strengths due to air inclusions. Further, the order of magnitude difference in the thermal expansion coefficient of the metal particles versus the typical polymer matrix [6] leads to thermomechanical hysteresis.

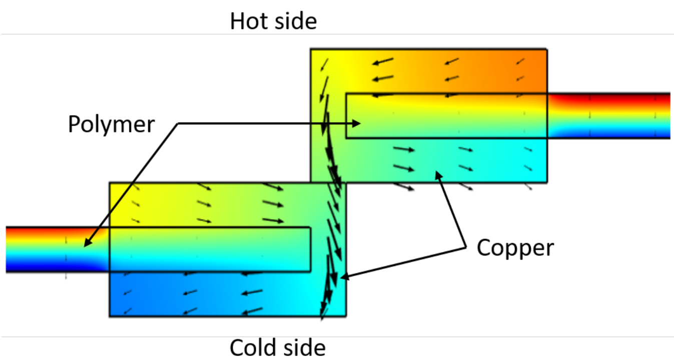

FIGURE 1: Simulation of shunted heat flow (shown by arrows) from hot side (exhaust gases at 400 K) to cold side (water at 300 K). Red (top) indicates hot temperature and blue indicates cold temperature. Hot side and cold side correspond to heat transfer coefficients of 10 W/m^2.K and 300 W/m^2.K respectively. Majority of the heat flux arrows pass through copper.

To overcome the above issues, we describe here a different approach: a macroscale metal-polymer hybrid that separates the heat conduction pathway between metal and polymer such that heat essentially flows in parallel circuits across the two materials. This specifically reduces the impact of the large thermal interfacial resistance between metal and polymer. In a tube formed from the material, heat conduction is short-circuited from the hot to the cold side across the HX walls through the metal while the polymer provides the mechanical scaffold for the HX tube. Figure 1 illustrates the basic idea behind the approach. The polymer strips act as a scaffold for an extended copper surface that is also formed from a thin foil. When the combination is subject to convection on the two sides, the heat flow lines indicate that the heat is shunted through the copper. This two-dimensional structure can be thought of as the surface of a three-dimensional hollow tube, which can be fabricated by wrapping polymer and copper strips together. For example, a helical wrapping of metal and polymer strips can be done in a roll to roll (R2R) process. More such configurations are discussed in detail in the following sections. The strategic placement of copper and polymer strips ensures that the overall heat transfer coefficient is not limited by the wall thermal resistance.

Two key challenges in this approach are (1) retaining the heat transfer pathways i.e. reasonable effective thermal conductivity and (2) maintaining thermomechanical strengths for safe operation. In a separate paper, [11] we discuss the first challenge in detail. In that work, through numerical simulations, we obtain copper-polymer geometries that achieve a viable wall thermal conductivity ~1 W/m.K at ~23% volume fraction of copper. The enhancement in thermal conductivity is around ~23% compare to all polymer heat exchangers. Computer simulations show that under the normal operating conditions of the heat exchanger, these hybrid pipes can withstand >200 psi internal pressures. In the current work, we explore solutions to overcome the second challenge: the critical problems of bonding the metal and polymer and metal to metal. Prior work has extensively investigated different methods of joining metals to polymers [12–17]. The high fluidity of adhesives and their ability to form strong bonds between specific metals and polymers under sufficient applied pressures is particularly useful in this work. Such bonding is also suited to the curved interfaces that are encountered in this work. Finally, the speed at which the bonding can be performed is an added advantage. Hence, we consider joining metal to polymer using adhesives (epoxy, acrylic and silicone). We further explore ultrasonic welding for joining metal to metal as a first step. Other choices such as laser and resistive welding will be explored in future work.

TABLE 1: Testing protocol followed in our experiments

Test type	Amplitude of "Single Ramp" test (mm)	Ramp slope (mm/sec)	Sampling frequency (ms)	Repetitions (n)	Material Thickness (1mil ≈ 25μm)	Joint dimensions
Adh-Peel	90	4.5	20	5	Cu – 1 mil, Poly – 2 mil	3 cm x 2.54 cm
Adh-Shear	5	0.2	10	5	Cu – 1 mil, Poly – 2 mil	5 cm x 2.54 cm
USW-Peel	35	1	10	4	Cu – 10 mil	8mm dia.
USW-Shear	8	0.3	10	10	Cu – 10 mil	8mm dia.
USW-Shear	8	0.3	10	10	Cu – 8 mil	8mm dia.

The paper is organized as follows. Various joining techniques for metal polymer hybrid heat exchangers are discussed. Section 2 describes the various configurations of strip geometries. We further discuss the materials used and the possible joining methods. Section 3 discusses the results obtained from the thermomechanical experiments conducted on samples made using these materials and methods. In Section 4, we conclude that the innovative joining techniques for metals polymer hybrids, presented here, are promising. This work paves way for realizing cost-effective manufacturing of heat exchangers for low grade waste heat recovery.

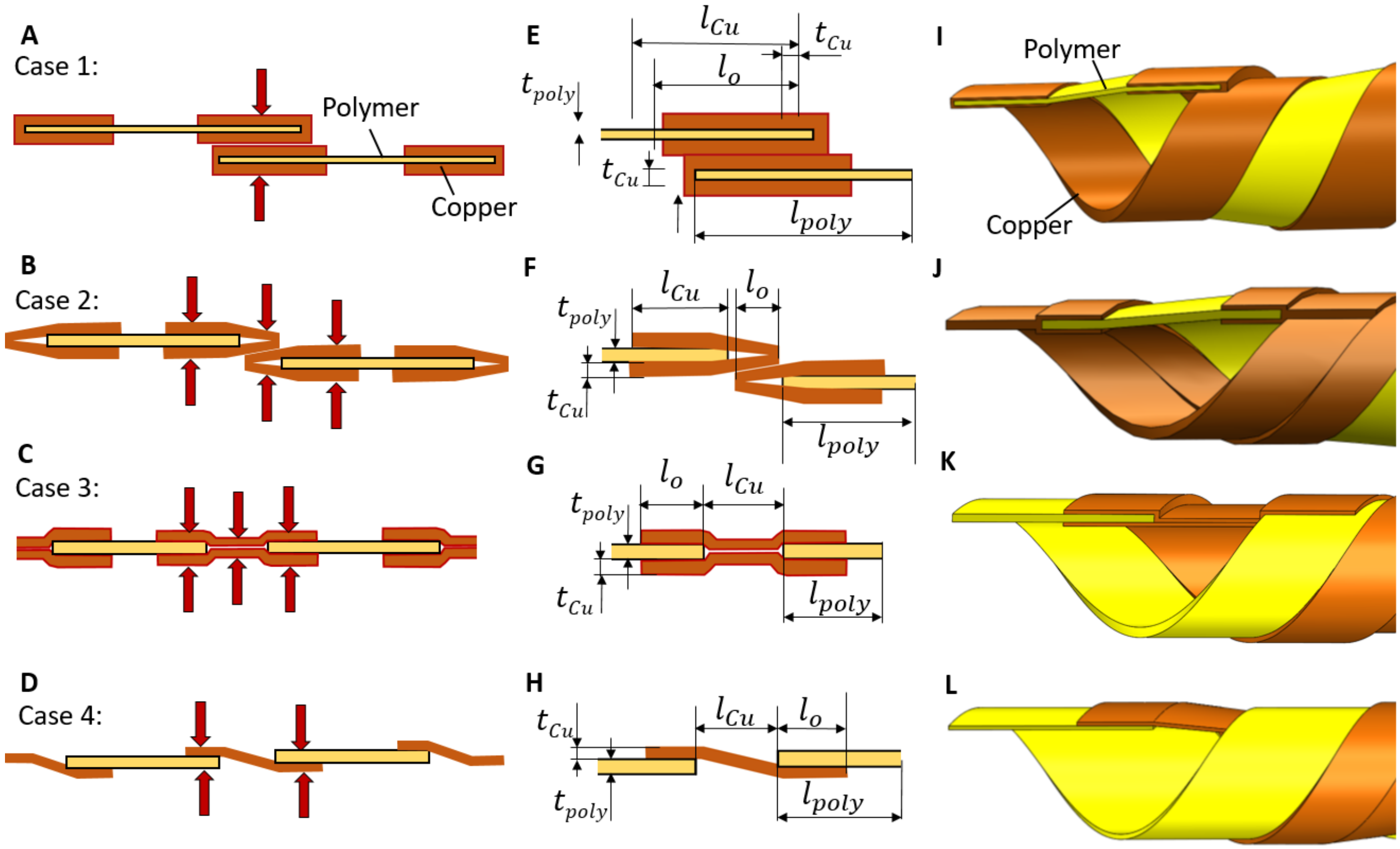

FIGURE 2: Different strip geometries of the hybrid heat exchanger. (A, E, I), (B, F, J), (C, G, K) and (D, H, L) are respective sets of figures for cases 1, 2, 3 and 4. Sub figures A, B, C and D are top wall cross-sections. Sub figures E, F, G, and H are unit cells labeled with important dimensions. Sub figures I, J, K and L are the 3-dimensional CAD models of the hybrid tubes. Solid red arrows indicate locations where joints are required. Metal/metal and metal/polymer joints are the possible joints.

2. JOINING TECHNIQUES AND TESTING

In the current study, materials under consideration are (1) Copper as the metal and (2) DuPont™ Kapton® HN film (a polyimide) as the polymer. Thickness of the polymer is 2 mil (~ 50 µm). Copper 1181 conductive tapes with a thickness of 1 mil (~ 25 µm) are used for adhesive joint tests and 110 Copper foil with a thickness of 10 mil (~ 250 µm) are used for USW joint tests. These materials meet ASTM B152 standards. Joints are described in subsection 2.2. In further sections the words metal and copper are used interchangeably. Copper is chosen for its high thermal conductivity (400 W/m.K) and polyimide for its high temperature stability (200 °C). Further, the linear thermal expansion coefficients of the materials are comparable (17 ppm/°C for copper and 20 ppm/°C for polyimide).

2.1 Tape Geometry and Various Joints

Figure 2 illustrates various tape geometries which can yield a HX tube upon proper procedural bonding. The red arrows in the figure indicate the places where joining is required. As discussed earlier, possible joining techniques include adhesive bonding and seam welding. The important geometric dimensions are the lengths (l_{Cu}, l_{poly}) and thicknesses (t_{Cu}, t_{poly}) of copper and polymer layers. The length of overlap (l_o) determines the relative positions of these layers.

Cases 1, 2 and 3 have both copper/copper and copper/polymer joints. Case 4 is much simpler and contains only copper/polymer joints. These joints when formed should hermetically seal a cylindrical tube. To make the metal/metal joints in a continuous process, we initially considered three welding techniques namely ultrasonic, laser and resistance seam welding. Laser welding is more challenging for joining copper to copper. This is because of the high thermal conductivity and high surface reflectivity of copper [13,14]. Ultrasonic welding (USW) is a fast and economic approach for joining copper to copper as well as copper to polymers [14]. We note that in general, USW is not associated with joining metals to polymers but can yield potential savings in operational costs. High heat generation is likely to be an issue in resistance welding of copper to copper in our designs because of the copper being adjacent to the polymer. The other joint, between the copper and the polymer was made using adhesive bonding (acrylic, epoxy and silicone).

The above joining techniques can be used to potentially realize the heat exchangers shown in the Fig. 2 (I, J, K, L). For largescale integrated production, these tubes can be made in a roll to roll process involving helical wrapping of copper and polymer strips and simultaneous application of joining methods. Metal-metal joints are easier to form and are typically stronger

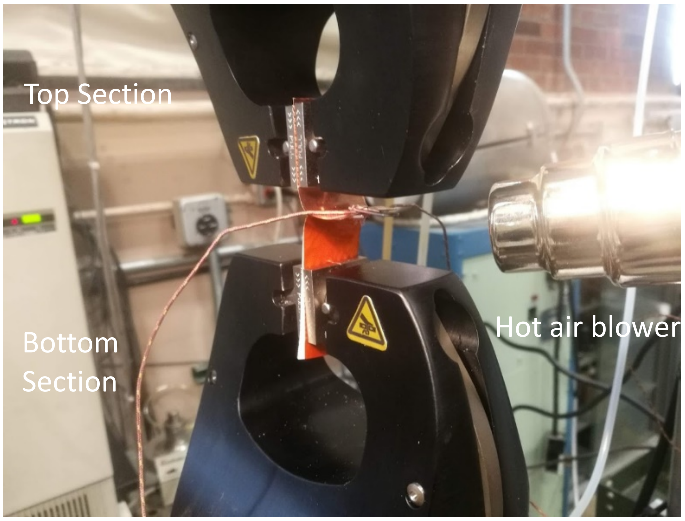

FIGURE 3: Tensile (peel) mode of testing. Top jaw clamps copper strip and bottom jaw clamps polymer strip.

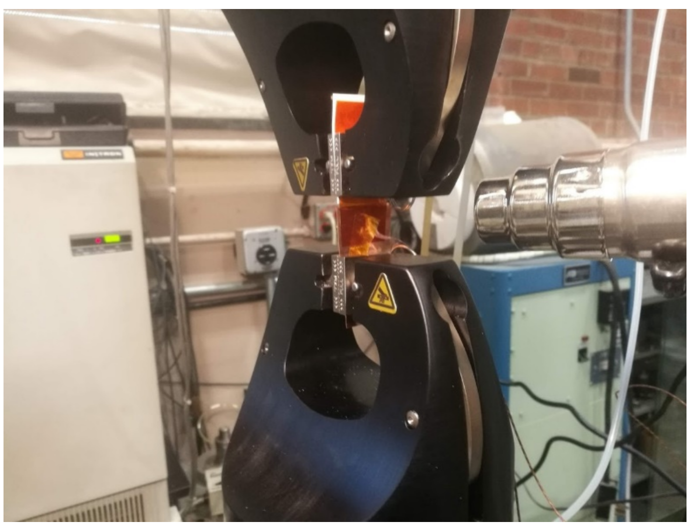

FIGURE 4: Shear mode of testing. Top jaw clamps copper strip and bottom jaw clamps polymer strip.

than joints between metals and polymers. It is obvious that copper/polymer joints play a limiting role in the structural integrity of the heat exchangers. Prior work [15,16] provides an in-depth analysis of fracture mechanics in metal polymer hybrid materials. Delamination is the primary mode of failure in these hybrid materials [17]. Two common modes of failure are considered in this paper: (1) Opening or Peel or Tensile or Mode 1 and (2) Shear or Mode 2. Peel strength is generally used to measure the bond strength of adhesive joints and is the average load per unit width of bond line required to separate bonded materials where the angle of separation is 180 degrees. It is usually denoted in N/cm or pounds/inch. In contrast, a shear load tends to produce a sliding failure on a material along a plane that is parallel to the direction of the force. It is usually denoted in MPa.

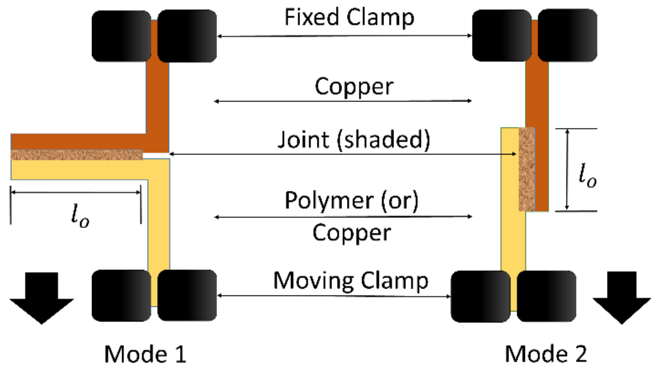

FIGURE 5: 2D block diagram of testing in Mode 1 and Mode 2. The joint region is l_0 x l_{poly} (1.5 cm x 2.54 cm). l_{poly} is measured into the plane of paper and same as l_{Cu}.

2.2 Testing

A Branson Ultraweld L20 Spot Welder was used in this study to perform USW. Energy mode and welding cycles were selected to reach the specified energy. USW is used for making metal/metal interface samples. The diameter of the weld spot is 8mm across all the samples. Epoxy (4540N) adhesives were obtained from Cotronics, Inc. Native adhesives present on the copper and polyimide foil tapes are acrylic and silicone respectively. These adhesives were used for making metal/polymer interface samples. The thickness of each adhesive is approximately 1.2 mil (~30 µm).

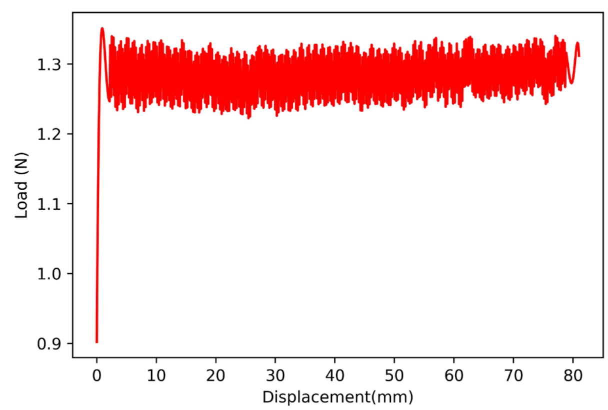

FIGURE 6: Illustrative load curve in peel tests for adhesive joints. This specific curve is for acrylic adhesive at 200°C. The average value of the dense oscillations is used to compute peel strength.

To measure the bond strength of both M/M and M/P joints, we performed thermomechanical tests on sample specimens made using these joining methods. Peel (Fig. 3) and Shear (Fig. 4) tests were performed on a high accuracy Instron universal testing machine (model 1332) with digital data output. Figure 5 shows the 2-dimensional block diagram of these thermomechanical tests. Since the heat exchanger is designed to perform in a hot air environment, these tests were performed at different air temperatures. A hot air blower (Tacklife, 1700W, 50-650°C, 250-500 L/min), was used to create the necessary experimental conditions. Two thermocouples were attached to the test specimen, one facing the hot air side and one on the other side of the sample. These thermocouples provided the surface temperature of the samples. They were mainly used to check the flow conditions (by calculating average temperature of the joint) across the different sets of experiments.

Table 1 shows the experimental conditions. It is important to note that the surface conditions and curing parameters affect the strength of adhesive bonds. For the sake of consistency, all adhesive joint samples were cured at room temperature for 24 hours under a positive pressure of approximately 650 gm-force per sample. Post curing was performed at 125°C for 90 minutes. This ensures the completion of any microstructural changes which occur at dissimilar surfaces.

3. RESULTS AND DISCUSSION

In this section, we present results from thermomechanical testing and discuss the implications.

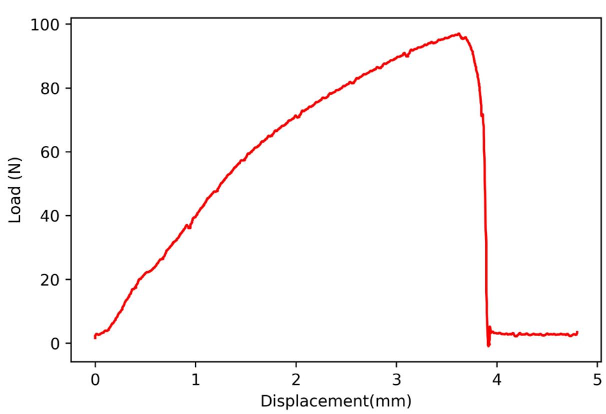

FIGURE 7: Illustrative load curve in shear tests for adhesive joints. This specific curve is for Epoxy adhesive at 150°C. Peak value of load is used to compute shear strength.

3.1 Metal/Polymer Joints - Adhesives

Figures 6 and 7 show typical load curves for the peel and shear tests respectively in metal-polymer adhesive joints. The maximum values of the peel strength and shear strength are reported in Figures 8 and 9. The error bars indicate the variance in repeated experiments. Both the peel and shear strengths of the adhesive joints decrease with increase in temperature, as expected. This can be attributed to the softening of the adhesives (essentially made of polymers) at higher temperatures. Acrylic is a thermoplastic material which melts and reflows at high

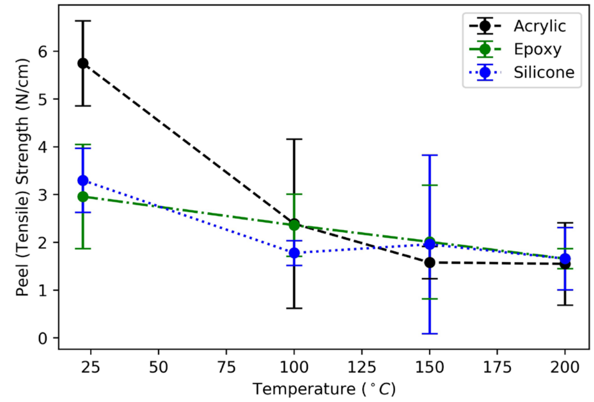

FIGURE 8: Peel strength plots for adhesive joints. We observe a general trend of decreasing strengths with temperature. The fall in the strengths is highest in Acrylic followed by Epoxy and Silicone in no particular order.

temperature. It has a superior peel strength that decreases rapidly with increase in temperature. Further acrylic degasses and produces poisonous fumes above 150 °C. Hence, it is not recommended for use in its current form. Silicone is another choice of bonding though the high variability and thus, poor reliability in bond strength, render it a poor choice. Epoxy is a thermoset polymer which forms a permanent rigid M/P bond which also provides structural strength in a cylindrical geometry. Epoxies appear to be a good choice based on these tests.

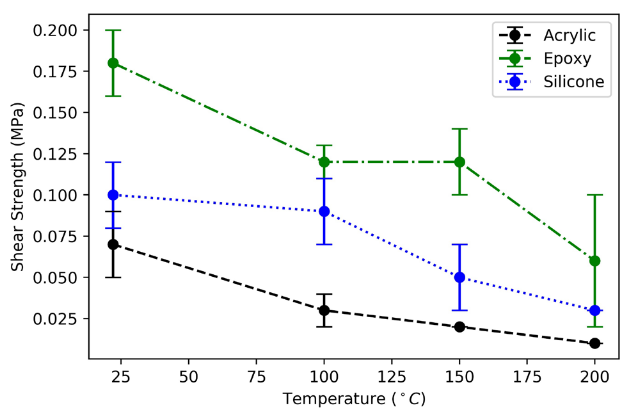

FIGURE 9: Shear strength plots for adhesive joints. We observe a general trend of decreasing strengths with temperature.

3.2 Metal/Metal Joints – Ultrasonic Welding

Figures 10 and 11 show typical load curves for the peel and shear tests respectively in metal to metal USW joints. The diameter of the weld spot is 8mm across all the samples. The error bars indicate the variance across experiments. The nature of the peel load curve can be explained by the mesh nature of the USW. Initially, the bonds break one strand segment after another resulting in an oscillatory trend in the strength-displacement curve. This trend is consistent across the samples and acceptable. We report the peel strength for spot welds in terms of peak load, consistent with literature. Peel strength can be calculated, for comparison with adhesive, by normalizing the peak force with the weld diameter of 8mm. Reporting this value in N/cm may not be the most appropriate measure because of the failure of joint in two successive modes, namely failure in mesh region and failure in heat affected zone.

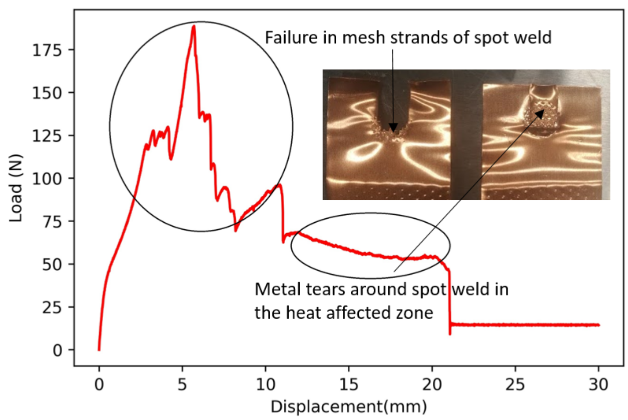

FIGURE 10: Illustrative load curve in peel tests for ultrasonic weld joints between two copper strips each with a thickness = 10 mil (~250 µm). The oscillatory nature is due to the sequential failure of strands in the mesh structure of the ultrasonic weld. In the later part of test, metal tears around spot weld in the heat affected zone. The inset picture is a sample after testing showing these types of failure. The maximum value of the load is used to compute peel strength.

We performed all these tests at room temperature (25 °C) only. This is mainly to measure the strengths relative to the adhesive joints. Welding was performed using a mix of weld amplitudes and weld times to further identify optimal welding conditions. Figure 12 shows the peel strength data. A simple calculation shows that the peel strength of M/M USW joints, on an average, is higher by two orders of magnitude, compared to the M/P adhesive joints. Figure 13 shows peak shear strength data for USW joints between copper strips each with a thickness of 10 mil (~ 250 µm). We observe that the weld time does not have a significant effect on the strength. However, higher weld amplitudes produce joints with higher shear strength with a peak at 50 µm. Figure 14 shows the results for similar tests on copper strips with thickness of 8 mil (~200 µm). There is a marked decrease in average strengths, from 14 MPa at 10 mil (~250 µm) to 11 MPa at this lower thickness. Overall, weld amplitude of 50 µm with a weld time of 0.6 s and higher thicknesses of copper are preferable for strong welds. For the purpose of forming tubes, the thickness is however limited due to the requirement for the strip to bend to form a curved surface.

4. CONCLUSION AND FUTURE WORK

In summary, we explored different configurations of a metal polymer hybrid heat exchanger. We presented joining techniques that can realize a variety of designs for pipe geometries. Thermomechanical tests were performed to estimate the bonding strengths of adhesive and USW joints. We find epoxy adhesives and ultrasonic welding as suitable joining methods for metal/polymer and metal/metal interfaces respectively. These results give impetus to a roll to roll process as a feasible manufacturing technology for producing metal polymer hybrid heat exchangers.

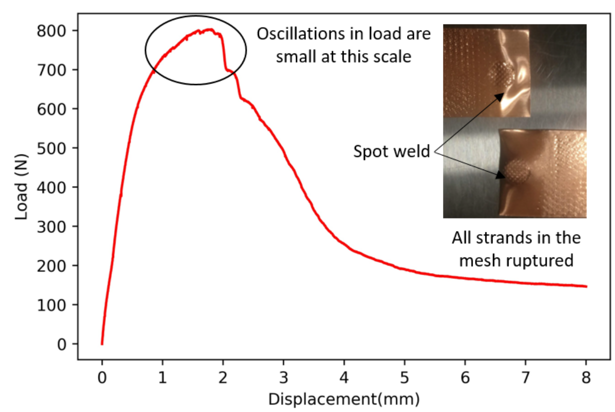

FIGURE 11: Illustrative load curve in shear tests for ultrasonic weld joints between two copper strips each with a thickness = 10 mil (~250 µm). Oscillations in load are small at this scale. The inset picture show a sample post testing. Peak load value is used to compute shear strength.

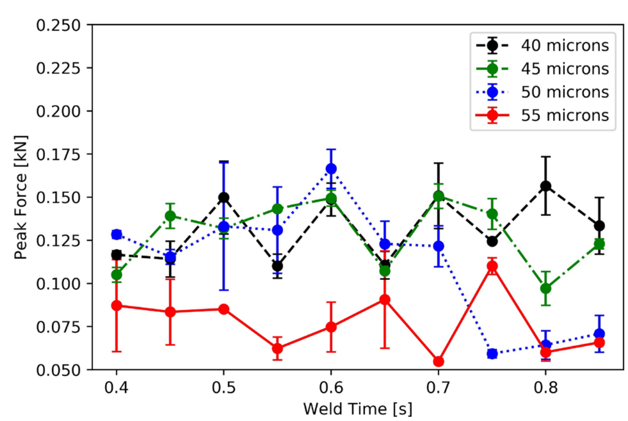

FIGURE 12: Peel strength of ultrasonic welds between copper strips of 10 mil (~250 µm) thickness. Tests were performed at room temperature (22 ˚C).

The adhesive strengths between metal and polymer strips are lower compared to metal/metal USW joints. Thus, they are the limiting interface for failure. Hence, further work is necessary to find mechanisms for strengthening adhesives. To determine scalability of the methods presented here, we must perform full factorial testing on a complete cylindrical heat exchanger with water and flue gas flow rates and inlet temperatures as variables. Efforts for making a desktop R2R manufacturing setup for producing helically wrapped heat exchangers are underway. We are also working to integrate the joining strategies presented in this paper within the R2R type setup.

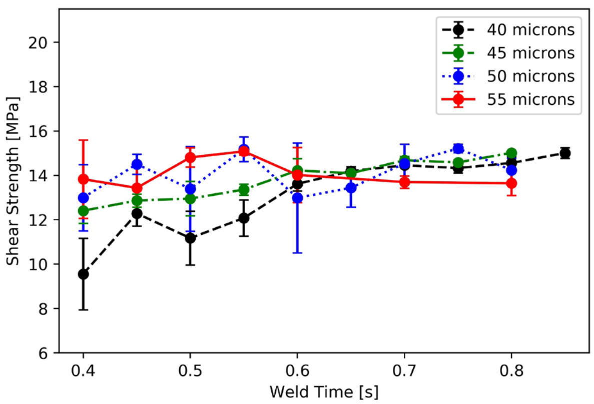

FIGURE 13: **Shear strength of ultrasonic welds between copper strips of 10 mil (~250 µm) thickness. The samples were made at 4 different wave amplitudes (40, 45, 50 and 55 µm). Tests were performed at room temperature (22 ˚C). Higher weld amplitudes yield better strengths on an average. We observe that weld times don't have a significant effect on strengths.**

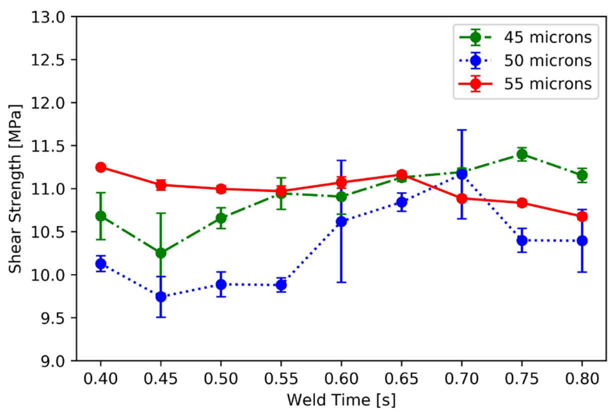

FIGURE 14: **Shear strength of ultrasonic welds between copper strips of 8 mil (~200 µm) thickness. The samples were made at 3 different wave amplitudes (45, 50 and 55 µm). Tests were performed at room temperature (22 ˚C)**

ACKNOWLEDGEMENTS
The authors gratefully acknowledge a research award from the Department of Energy, US (DE-EE0008312).

REFERENCES

[1] BCS, Incorporated, 2008, "Waste Heat Recovery: Technology and Opportunities in U.S. Industry."

[2] Thekdi, A., and Nimbalkar, S. U., 2015, "Industrial Waste Heat Recovery-Potential Applications, Available Technologies and Crosscutting R&D Opportunities. Oak Ridge National Lab."

[3] Awad, M., 2011, *Heat Transfer - Theoretical Analysis, Experimental Investigations and Industrial Systems*, InTech Open Access.

[4] Hussain, A. R. J., Alahyari, A. A., Eastman, S. A., Thibaud-Erkey, C., Johnston, S., and Sobkowicz, M. J., 2017, "Review of Polymers for Heat Exchanger Applications: Factors Concerning Thermal Conductivity," Applied Thermal Engineering, **113**(C), pp. 1118–1127.

[5] Nurazreena, Hussain, L. B., Ismail, H., and Mariatti, M., 2006, "Metal Filled High Density Polyethylene Composites – Electrical and Tensile Properties," Journal of Thermoplastic Composite Materials, **19**(4), pp. 413–425.

[6] Aymonier, C., Bortzmeyer, D., Thomann, R., and Mülhaupt, R., 2003, "Poly(Methyl Methacrylate)/Palladium Nanocomposites: Synthesis and Characterization of the Morphological, Thermomechanical, and Thermal Properties," Chemistry of Materials, **15**(25), pp. 4874–4878.

[7] Roy, A., Bougher, T. L., Geng, R., Ke, Y., Locklin, J., and Cola, B. A., 2016, "Thermal Conductance of Poly(3-Methylthiophene) Brushes," ACS Applied Materials & Interfaces, **8**(38), pp. 25578–25585.

[8] Wang, X., Ho, V., Segalman, R. A., and Cahill, D. G., 2013, "Thermal Conductivity of High-Modulus Polymer Fibers," Macromolecules, **46**(12), pp. 4937–4943.

[9] Choy, C. L., Wong, Y. W., Yang, G. W., and Kanamoto, T., 1999, "Elastic Modulus and Thermal Conductivity of Ultradrawn Polyethylene," Journal of Polymer Science Part B: Polymer Physics, **37**(23), pp. 3359–3367.

[10] Tavman, I. H., 1996, "Thermal and Mechanical Properties of Aluminum Powder-Filled High-Density Polyethylene Composites," Journal of Applied Polymer Science, **62**(12), pp. 2161–2167.

[11] Rajagopal, M., Chang, H. C., Man, T., Kuntumalla, G., Gelda, D., Meng, Y., Sundar, S., Zhao, H., Salapaka, S., Shao, C., Ferreira, P., Miljkovic, N., and Sinha, S., 2019, "Designing High Thermal Conductivity Pipes from Roll-to-Roll Processed Copper Polymer Strips," Manuscript in preparation for International J. Heat Mass Transfer

[12] Escaig, B., 1993, "Binding Metals to Polymers. A Short Review of Basic Physical Mechanisms.," Journal de Physique IV Colloque, **03 (C7)**, pp. C7-753-C7-761.

[13] Martinsen, K., Hu, S. J., and Carlson, B. E., 2015, "Joining of Dissimilar Materials," CIRP Annals, **64**(2), pp. 679–699.

[14] Meng, Y., Peng, D., Nazir, Q., Kuntumalla, G., Rajagopal, M., Chang, H. C., Zhao, H., Sundar, S., Ferreira, P., Sinha, S., Miljkovic, N., Salapaka, S., and Shao, C., 2019, "Ultrasonic Welding of Soft Polymer and Metal: A Preliminary Study," Erie, PA.
[15] Fafenrot, S., Grimmelsmann, N., Wortmann, M., and Ehrmann, A., 2017, "Three-Dimensional (3D) Printing of Polymer-Metal Hybrid Materials by Fused Deposition Modeling," Materials, **10**(10:1199).
[16] Moody, N. R., Reedy, E. D., Corona, E., Adams, D. P., Friddle, R. W., Kennedy, M. S., Cordill, M. J., and Bahr, D. F., 2012, "Copy of Deformation and Delamination in Polymer Metal Thin Film Structures," San Diego, CA.
[17] Al-Okaily, A., 2015, "Laser-Driven Micro-Transfer Printing for MEMS/NEMS Integration," University of Illinois at Urbana-Champaign.